

# Preparation of CuPc/RGO Nanocomposites and Their Electrocatalytic Behaviors for Oxygen Reduction Reaction

Guofang Zuo<sup>1</sup>, Peng Wang<sup>1</sup>, Zhifeng Li<sup>1</sup> and Jiandong Yang<sup>2</sup>

<sup>1</sup>College of Chemical Engineering and Technology, Tianshui Normal University, Tianshui 741000, P. R. China

<sup>2</sup>Department of Biology and Chemistry, Longnan Normal College, Chengxian 742500, P. R. China

Received: August 18, 2016, Accepted: October 27, 2016, Available online: December 05, 2016

**Abstract:** In this paper, copper phthalocyanine/reduced graphene oxide (CuPc/RGO) nanocomposites were synthesized by aromatic  $\pi$ - $\pi$  stacking interaction and well characterized by scanning electron microscopy (SEM) and fluorescence spectrometry. The composites were modified on the surface of glass carbon electrode (GCE) and their electrochemical behaviors of CuPc/RGO for electrocatalytic oxygen reduction reaction (ORR) were studied by cyclic voltammetry (CV). The study showed when the mass ratio of RGO to CuPc in composite achieved 1:1, the composite film performed excellent electrocatalytic activity towards the ORR.

**Keywords:** copper phthalocyanine (CuPc); reduced graphene oxide (RGO); nanocomposites; modified electrodes; electrocatalytic ORR

## 1. INTRODUCTION

Fuel cell is regarded as an effective and promising tool to solve environmental and energy problems [1-3]. The oxygen reduction reaction (ORR) reaction at the cathode in fuel cell sustained by oxygen or air plays critical rule for efficiently energy transformation. In general the ORR essentially needs catalysts to accelerate the process and realize high reaction efficiency. Among many catalysts developed over the past decades, Pt has shown the best catalytic performance. But its high cost has hampered its large-scale application and therefore seeking abundant and cheap substitutes for Pt is very necessary and important from the point of view of substantial development. Now various non-noble metals and functionalized carbon materials have been tested as catalysts for the ORR [4,5]. Among the non-noble metal catalysts, Fe [6], Co [7] and Mn [8] are the most studied materials. Besides, Cu-based materials to catalyze the ORR have also been developed rapidly.

Current researchs about Cu-based catalysts focuses on reducing overpotential and increasing onset potential of ORR. Gewirth [9,10] prepared Cu complexes of 2,2'-dipicolylamine (DPA) and tris-(2-pyridylmethyl)-amine (TPA) and tested them as electrocatalysts for the ORR to study the effect of multinuclearity on the ORR. These studies highlight the viability of Cu-DPA/Cu-TPA complexes serve as guides for designing future laccase models. Synthetic Cu complexes exhibit rich reactivity toward O<sub>2</sub> and have

the lowest ORR overpotential at pH 1 or 7. Kamiya [11] synthesized copper-modified covalent triazine frameworks (CTF) hybridized with carbon nanoparticles (Cu-CTF/CPs) as efficient electrocatalysts for the ORR in neutral solutions. The ORR onset potential of the synthesized Cu-CTF/CP was 810 mV, the highest reported value at neutral pH for Cu-based electrocatalysts. Cu-CTF/CP also displayed higher stability than a Cu-based molecular complex at neutral pH during the ORR. This work may provide a new platform for the synthesis of durable non-noble-metal electrocatalysts for various target reactions. Kamiya [12] also reported a novel copper-based oxygen reduction electrocatalyst by heat treating a mixture of reduced graphene oxides (RGO) and a Cu complex of 3,5-diamino-1,2,4-triazole. In neutral solutions, the catalyst exhibited efficient electrocatalytic activity for ORR, with an onset potential of 790 mV. More importantly, the catalyst possesses high stability due to the anchoring of active Cu-sites into the graphene substrate via the Cu-N coordination bonds. Wang [13] prepared a series of transition-metal phthalocyanines (TMPc) supported on graphitized carbon black (TMPc/GCB, TM: Fe, Co, Ni and Cu) as ORR electrocatalysts via  $\pi$ - $\pi$  interaction and self-assembly. It was found that TMPc was coated on graphitized carbon black with non-aggregated morphology. To better elucidate the ORR catalytic mechanism for TMPc/GCB, researchers employed DFT calculations and drew the following conclusions: (i) O<sub>2</sub> adsorption is the major step to determine the ORR catalytic activity; (ii) the way of O<sub>2</sub> adsorbed on TMPc is the key point affecting the Tafel slope;

\*To whom correspondence should be addressed: Email: zogofn@126.com

(iii)  $\text{H}_2\text{O}_2$  desorption determines the transfer electron number and (iv) the OH<sup>-</sup> desorption and the central metal atom removal together leads to the catalysts less durable.

From the above research, we find Cu-based materials have exhibited excellent electrocatalytic activities for ORR [14], but relatively few studies examine their ability to catalyze the reduction of dioxygen to water [15]. From a technical standpoint, the key to fuel cell viability is efficient mediation of the ORR to water:  $\text{O}_2 + 4\text{e}^- + 4\text{H}^+ \rightarrow 2\text{H}_2\text{O}$ . This  $4\text{e}^-$  reduction is almost critically relevant to all fuel cells. Therefore, in this work, we hydriized copper phthalocyanine (CuPc), a good electrocatalytically active material with reduced graphene oxide (RGO) sheets via strong  $\pi$ - $\pi$  interaction. And these CuPc/RGO composites were investigated for electrocatalytic ORR.

## 2. EXPERIMENTAL

### 2.1. Reagents

All reagents used in this work were of analytical grade and employed without further purification. Graphite was purchased from Sinopharm Chemical Reagent Co. (Shanghai, China). Hydrazine solution (85%) was provided by Beijing Chemicals Inc (Beijing, China). All reagents are analytical grade. Water was distilled from an all-quartz still and high pure oxygen were used for aeration.

### 2.2. Apparatus

Fluorescence spectra were recorded with a Shimadzu RF-5301PC Fluorescence Spectrophotometer (Shimadzu, Japan). Electrochemical measurements was conducted on a CHI 832 Electrochemical workstation (CHI, USA). The morphologies of RGO and CuPc/RGO were examined with a JSM-671F cold field emission scanning electron microscope (SEM, Electro-optical company, Japan). Acidity was measured by a PHS-3B Precision pH Meter (Shanghai, China), and all sonication was done using a KQ-100 Ultrasonic Cleaner (Kunshan, China).

### 2.3. Preparation of graphene (RGO)

A modified Hummers [16,17] method was utilized to synthesize the graphene oxide. Hydrazine hydrate was added into graphene oxide drop by drop, and then reacted at 80 °C for 24h. After cooling to room temperature, the solid was filtered, subsequently washed with methanol and distilled water, and dried to obtain graphene (RGO).

### 2.4. Synthesis of CuPc

Urea (0.092 mol), phthalic anhydride (0.018 mol), copper (II) chloride (0.005 mol), and ammonium molybdate (0.0596 mol) were ground for 30 min in an agate mortar. The mixture was put into a flask and wetted with distilled water (5 ml). It was then heated in a microwave oven at 600 W for 5 min. The crude product was purified by washing in sequence with hot water (70 °C), 6 M HCl, 1 M NaOH, and with hot water again followed by filtration. After these steps, the pigment was washed with ethanol and filtered until the filtrate was colorless. The resulting pigment was dried in an oven at 100 °C.

### 2.5. Preparation of CuPc/RGO

The preparation of CuPc/RGO was as follows: dichloromethane as the solvent, 5 mg/ml CuPc solution and 5 mg/ml RGO suspen-

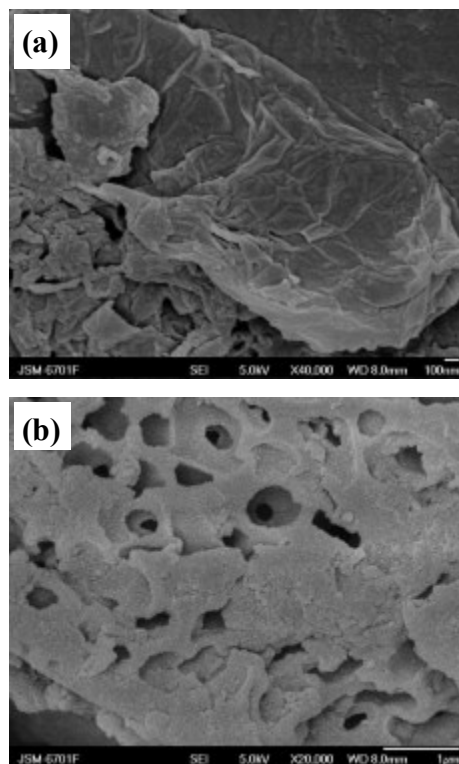


Figure 1. SEM image of RGO (A) and CuPc/RGO composites (B).

sion were mixed together. During ultrasonication, ethanol was added dropwise to the mixture until the liquid became clear. The nanocomposite was collected by filtration, washed with water and ethanol and dried in vacuum (80 °C).

### 2.6. Modification of the electrode

Prior to modification, the glass carbon electrode was polished with 1.0, 0.3, and 0.05  $\mu\text{m}$  alumina slurry, rinsed thoroughly with ultrapure water and ethanol, and dried with nitrogen, then washed successively with 1:1 nitric acid, acetone, and ultrapure water in an ultrasonic bath and dried in air. 1 mg CuPc/RGO nanocomposite was dispersed in 1ml DMF under ultrasonication for 1 h. A certain amount of suspended droplets applied to the polished glass carbon electrode (GCE) surface, and then dried at room temperature. Finally, 0.3% nafion solution was dropped on the CuPc/RGO/GCE surface.

### 2.7. Electrochemical measurement

Cyclic voltammetry measurements (CVs) were carried out with a CHI 832 electrochemistry workstation in 0.1 M different pH solution with a conventional three-electrode system comprised of a platinum wire as the auxiliary electrode, an Ag/AgCl as the reference electrode and the modified GCE as working electrode at a appropriate potential range.

## 3. RESULTS AND DISCUSSION

### 3.1. Characterization of CuPc/GR nanocomposites

The morphology of RGO and CuPc/RGO nanocomposites were

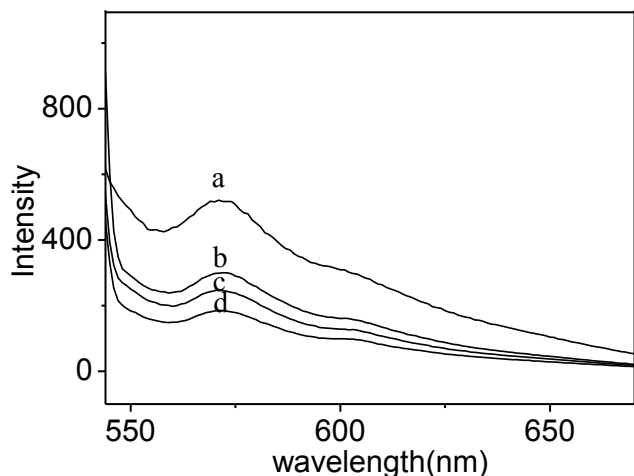


Figure 2. Fluorescence spectrometry of CuPc (a) and CuPc/RGO composites, the mass ratio of CuPc and RGO in composite is 10:1 (b), 1:10 (c), 1:1 (d).

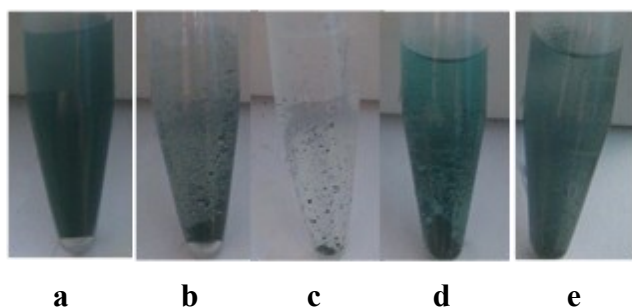


Figure 3. Image of CuPc/RGO dispersing in DMF (A),  $\text{CH}_2\text{Cl}_2$  (B),  $\text{H}_2\text{O}$  (C),  $\text{CH}_3\text{CH}_2\text{OH}$  (D),  $\text{CHCl}_3$  (E).

characterized by scanning electron microscopy (SEM). Fig. 1A show the typical layered sheets structure of RGO with a rippled morphology of the flake-like shapes randomly packed in stacked structures which demonstrated that graphene sheet structure was obtained. Furthermore, the adsorption of CuPc on the RGO surface can be seen clearly in SEM images and indicate forming a film of homogenous surface morphology. The strong attractive forces between RGO sheets and CuPc molecules, due to  $\pi$ - $\pi$  interaction, lead to composite formation. As shown in Fig. 1B, it can be seen that a film of CuPc with layered and wrinkled structure resides on the surface of the RGO sheets. The layered structures appear rougher than the morphology of pure RGO, indicating that CuPc has been successfully combined onto the surface of RGO. CuPc/RGO nanocomposites are beneficial for the fabrication of catalysis platforms due to their structure which provides a large surface area for further immobilization of various molecules.

Fluorescence spectrometry of CuPc/RGO nanocomposites were recorded to examine the electronic interactions of CuPc and RGO (Fig. 2). CuPc showed the typical fluorescence spectrometry of metallophthalocyanines and had a strong fluorescence peak at 570

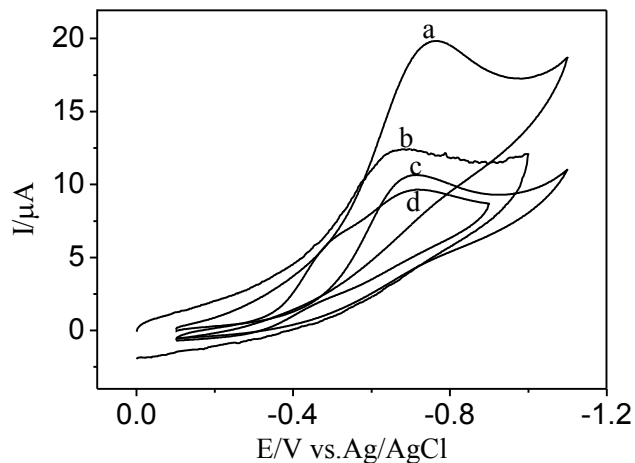


Figure 4. CVs of CuPc/RGO/nafion/GCE (a), RGO/nafion/GCE (b), CuPc/nafion/GCE (c) and nafion/GCE (d) in 0.1 M PBS (pH=7) containing saturation oxygen, dispensing volume is  $5\mu\text{l}$ ; scan rate  $50\text{ mV s}^{-1}$ .

nm. But when CuPc combined with RGO. We could observe distinctly luminescence quenching of CuPc, which reveals that there is a strong interaction between the excited state of CuPc and RGO in the hybrids. The fluorescence quenching of the excited CuPc may be due to its photoinduced electron transfer or energy transfer to RGO, which acts as a charge sink due to its conjugated network. This is a further evidence of the synthesis of CuPc/RGO. By comparison, quenching phenomenon is extremely obvious when mass ratio in composite is 1:1. This was consistent with the former report [18-21].

### 3.2. Selection of dispersion

CuPc/RGO was tested for dissolution respectively in DMF,  $\text{CH}_2\text{Cl}_2$ ,  $\text{H}_2\text{O}$ ,  $\text{CH}_3\text{CH}_2\text{OH}$ ,  $\text{CHCl}_3$  solution under ultrasonication, then stand for several days at room temperature (Fig. 3). By comparison, we found that the CuPc/RGO composites became clear and transparent and dissolved in DMF. It is well known that CuPc easily dimerizes in water to form non photoactive H aggregate whereas it can not dimerize in DMF [22,23]. So in this study, DMF was picked as the solvent, in which CuPc/RGO is well dissolved.

### 3.3. Electrochemical behaviors of CuPc/RGO

CVs was employed for investigating the electrochemical behavior of molecular oxygen at different electrodes (Fig. 4). In 0.1 M PBS buffer solution (pH=7.0), all modified electrodes displayed a reduction peak current around  $-0.7\text{ V}$ , suggesting that electron transfer was realized. The CuPc/RGO/nafion/GCE showed the largest reduction peak current compared to the other electrodes. And we didn't find the ORR activities in the absence of  $\text{O}_2$ . The electrocatalytic effects of CuPc/RGO composites on the saturation oxygen were likely attributed to high surface area which made electron transfer rate increase significantly. In addition, the high conductivity of graphene is also responsible for the increased current. Electrons can travel without being scattered off course by lattice imperfections and foreign atoms in graphene due to the high

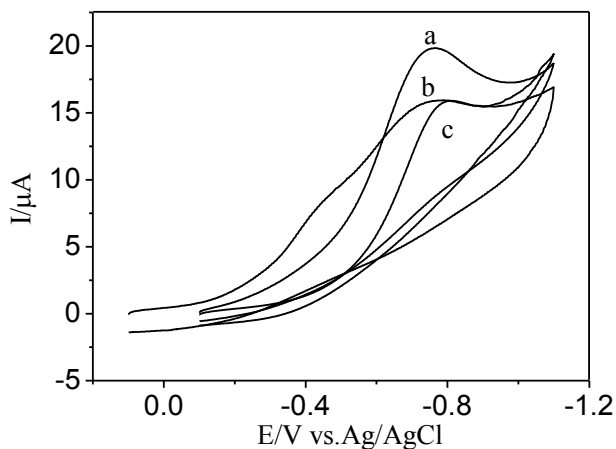


Figure 5. CVs of the CuPc/RGO/nafion/GCE in 0.1 M PBS (pH=7.0) containing saturation oxygen with different mass ratio of CuPc and RGO in composite: 1:1 (a), 1:10 (b) and 10:1 (c); dispensing volume is 5  $\mu\text{L}$ ; scan rate 50  $\text{mV s}^{-1}$ .

quality of its crystal lattice. The conduction electrons of graphene move much faster and as if they had far less mass than the electrons that wander about through ordinary metals and semiconductors [24]. The catalytic ability of the composite have enhanced to molecular oxygen by interaction of two materials. These two factors mentioned above make that the CuPc/RGO composite show excellent electrocatalytic properties for dioxygen reduction.

Numerous studies reported the usage of graphene-supported phthalocyanines (porphyrins) or their metal compounds as efficient electrocatalysts for dioxygen reduction [25-29]. These nanocomposites revealed certain degree of electrocatalytic activity towards dioxygen reduction. In alkaline medium, almost all electrocatalysts established a pathway of 4-electron transfer reactions. But the preparation of these nanocomposites were comparatively complicated compared with our complex which is synthesized by the simple  $\pi$ - $\pi$  conjugate interaction and effective method to improve the electrocatalytic activity of CuPc for combination with RGO. Electrochemical reduction/solvothetical/covalence combine have been made to prepare compounds in different literatures.

### 3.4. Selection of optimization condition

Fig. 5 shown the CVs of the CuPc/RGO/nafion/GCE in 0.1 M PBS (pH=7.0) containing saturation oxygen with different mass ratio of CuPc and RGO in composite. It can be seen that reduction peak potential for different mass ratio remains unchanged basically. By contrary, the significant changes in current intensity take place. When the mass ratio of CuPc to RGO in composite is 1:1, it can be observed that the reduction peak currents was larger than the others. It may be due to the CuPc can be dispersed uniformly and did not gathered at RGO surface, which promote the electron transfer effectively under this mass ratio. A further experiment was made.

Reduction peak currents are greatly influenced by the amount of CuPc/RGO deposited on the surface of glassy carbon electrode. When 5  $\mu\text{L}$  of CuPc/RGO suspension is deposited on the surface of GCE, results show that the reduction peak current and peak potential of dioxygen are ideal for ORR when the concentration of CuP-

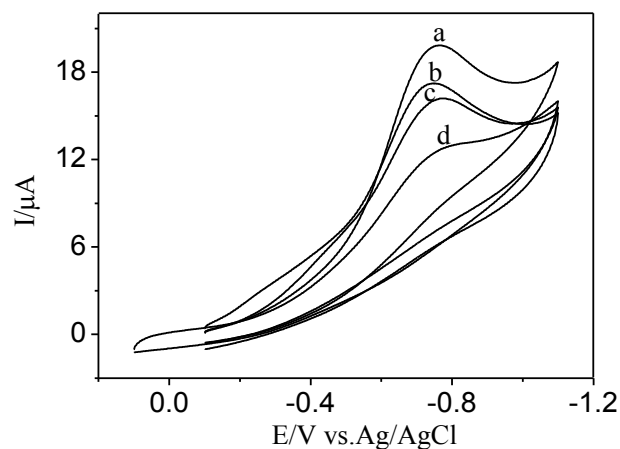


Figure 6. CVs of CuPc/RGO/nafion/GCE in 0.1 M PBS (pH=7.0) containing saturation oxygen with different dispensing volume. 5  $\mu\text{L}$  (a), 10  $\mu\text{L}$  (b), 15  $\mu\text{L}$  (c) and 3  $\mu\text{L}$  (d); mass ratio of CuPc and RGO in composite is 1:1; scan rate is 50  $\text{mV s}^{-1}$ .

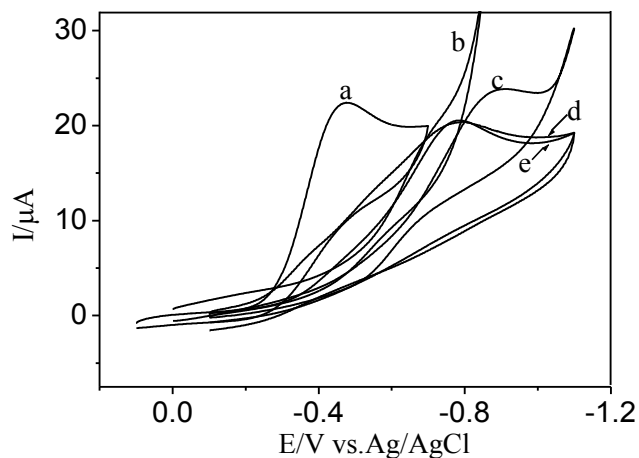


Figure 7. CVs of CuPc/RGO/nafion/GCE in the presence of saturation oxygen with different pH of buffer solution (0.1M): pH 12.0 (a), pH 1.0 (b), pH 4.0 (c), pH 10.0 (d) and pH 7.0 (e); mass ratio of CuPc and RGO in composite is 1:1, dispensing volume is 5  $\mu\text{L}$ , scan rate is 50  $\text{mV s}^{-1}$ .

c/RGO is 1 mg/ml (Fig. 6). Casting volume of CuPc/RGO greater than 5  $\mu\text{L}$  causes the CuPc/RGO coating on electrode surface excessively thick. Due to the excessive thickness of CuPc/RGO coating, the catalyst can not be employed efficiently and the diffusion of catalytic substrate to electrode surface becomes more difficult, thus the reduction peak current is reduced and the peak potentials is more negative. Moreover, when the casting volume of CuPc/RGO is less than 5  $\mu\text{L}$ , the catalyst can not cover fully on the surface of electrodes, also cause the reduction peak current of dioxygen reduced. So, in our experiments, 5  $\mu\text{L}$  of CuPc/RGO suspension with a concentration of 1 mg/ml was used in the preparation of CuPc/RGO-modified electrode.

In most cases, the solution pH is an important influence factor on

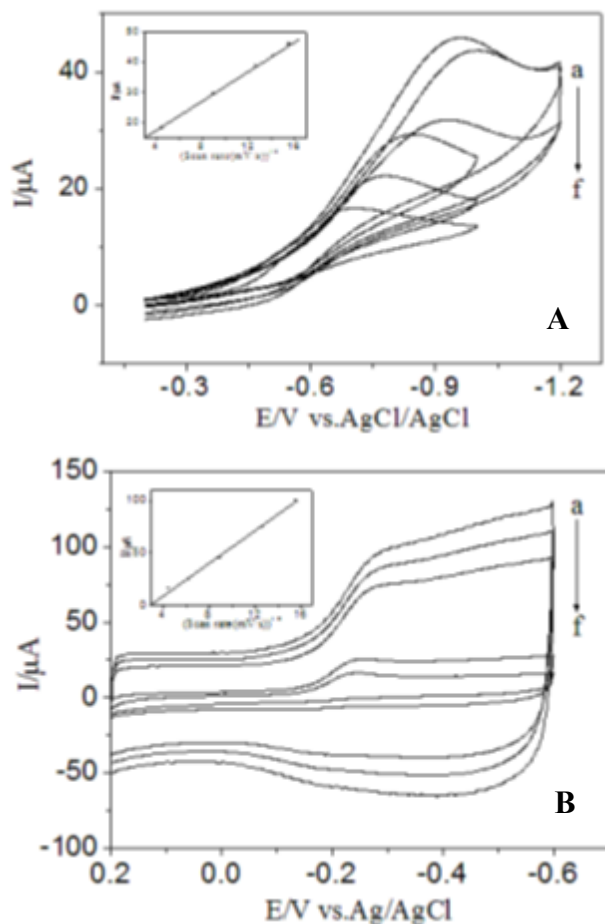


Figure 8. CVs of CuPc/RGO/nafion/GCE on different scan rate in the presence of saturation oxygen (A. 0.1 M  $H_2SO_4$ , pH=1.0; B. 0.1 M NaOH, pH=12) (af): 240, 200, 160, 80, 40, 20 mV/s, insert: current intensity vs  $v^{1/2}$ .

the electrochemical reaction. Cyclic voltammetry was carried out to characterize influence of solution pH on electrochemical behavior of saturated oxygen at CuPc/RGO/nafion/GCE. Fig. 7 showed the dependence of reduction peak of oxygen with different pH solution:  $H_2SO_4$  solution (pH=1.0), NaAc-HAc (pH=4.0), PBS (pH=7),  $Na_2CO_3$ -NaHCO<sub>3</sub> (pH=10), NaOH (pH=12). Obviously, under acidic conditions, the reduction peak potential (about -0.75V) is more negative than neutral solution. Conversely, the reduction peak potential (about -0.45V) is more positive in alkaline. In addition, the difference of reduction peak current is also greater in alkaline.

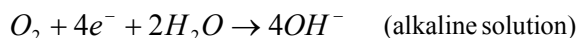
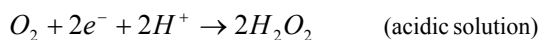
Relationship between different scan rate and reduction peak current intensity of CuPc/RGO/nafion/GCE were investigated further by CVs in 0.1M NaAc-HAc (pH=4.0) and 0.1M NaOH (pH=12.0) (Fig. 8). As scan rate in the range of 20  $mV s^{-1}$  to 240  $mV s^{-1}$ , the reduction peak current intensity increased continuously. Current intensity increased linearly with square root of scan rate is a liner relationship. This study suggested that the electrocatalytic processes were controlled by molecular oxygen diffusion on the surface of modified electrode [30]. For a typical irreversible reaction, the

relationship between peak current and scan rate was as follows [31-33].

$$i_p = 0.4958nFAC_0 \left( \frac{cn_a F}{RT} \right)^{\frac{1}{2}} v^{\frac{1}{2}} D_0^{\frac{1}{2}} \quad (1)$$

$$\Delta E_p = \frac{1.15RT}{cn_a F} \quad (2)$$

$\Delta E_p$  is the peak potential change when the scan rate increases 10-fold. Other symbols have their usual significance. The number of electrons  $n$  for the reduction dioxygen could be calculated as 2.05 for CuPc/RGO/Nafion/GCE in 0.1M NaAc-HAc (pH=4.0) and 4.13 in 0.1 M NaOH (pH=12.0). These facts concluded that under catalysis of CuPc/RGO, dioxygen reaching the surface of electrode by diffusion was reduced mainly through a 2-electron process to  $H_2O_2$  in acidic solution, and a 4-electron process to water in alkaline solution. Electron transfer process was concerned with proton in acidic condition. Conversely, the oxygen can reduced easily under alkaline condition. And molecules oxygen were reduced directly to water by acquirement of the 4 electrons. The reduction equation was as follows.



#### 4. CONCLUSIONS

In summary, A new type of CuPc/RGO nanocomposites were synthesized by a simple  $\pi$ - $\pi$  conjugate interaction, with CuPc adsorbed/inserted on/in RGO sheets. The prepared CuPc/RGO nanocomposites modified electrode (CuPc/RGO/nafion/GCE) exhibited enhanced electrocatalytic activity towards dioxygen in the mass ratio of CuPc and RGO in composite is 1:1. Under catalysis of CuPc/RGO, oxygen molecular reached the electrode by diffusion with a 2-electron process in acidic solution and a 4-electron process in alkaline solution. During the past decades, fuel cells have been widely investigated and considered as one of most promising fields for attaining energy in the near future. Due to the feature of high stability, catalytic efficiency, low pollution, CuPc/RGO nanocomposite materials can be useful for electrochemical catalytic with better performance.

#### 5. ACKNOWLEDGEMENTS

This project were supported by the Natural Science Foundation of China (No. 21465021, 21463023), the Natural Science Foundation of Province of Gansu, China (No. 1208RJZE139) and the "QingLan" Talent Engineering Funds of Tianshui Normal University.

#### REFERENCES

- [1] M. Armand, J. M. Tarascon, Nature, 451, 652 (2008).
- [2] J. Potocnik, Science, 315, 810 (2007).
- [3] C. Du, X. H. Gao, W. Chen, Chinese Journal of Catalysis, 37, 1049 (2016).

- [4] K. P. Gong, F. Du, Z. H. Xia, M. Durstock, L. M. Dai, *Science*, 323, 760 (2009).
- [5] Y. G. Li, W. Zhou, H. L. Wang, L. M. Xie, Y. Y. Liang, F. Wei, J. C. Idrobo, S. J. Pennycook, H. J. Dai, *Nat. Nanotechnol.*, 7, 394 (2012).
- [6] M. Lefevre, E. Proietti, F. Jaouen, J. P. Dodelet, *Science*, 324, 71 (2009).
- [7] Y. Y. Liang, Y. G. Li, H. L. Wang, J. G. Zhou, J. Wang, T. Regier, H. J. Dai, *Nat. Mater.*, 10, 780 (2011).
- [8] T. Takashima, K. Hashimoto, R. Nakamura, *J. Am. Chem. Soc.*, 134, 1519 (2012).
- [9] E. C. M. Tse, D. Schilter, D. L. Gray, T. B. Rauchfuss, A. A. Gewirth, *Inorg. Chem.*, 53, 8505 (2014).
- [10] M. A. Thorseth, C. S. Letko, E. C. M. Tse, T. B. Rauchfuss, A. A. Gewirth, *Inorg Chem.* XXX (XXXX) XXX.
- [11] K. Iwase, T. Yoshioka, S. Nakanishi, K. Hashimoto, K. Kamiya, *Angew. Chem.*, 127, 11220 (2015).
- [12] H. Koshikawa, S. Nakanishi, K. Hashimoto, K. Kamiya, *Electrochimica Acta*, 180, 173 (2015).
- [13] Z. P. Zhang, S. X. Yang, M. L. Dou, H. J. Liu, L. Gu, F. Wang, *RSC Adv.*, 6, 67049 (2016).
- [14] M. M. Liu, R. Liu, W. Chen, *Biosens Bioelectron.*, 45, 206 (2013).
- [15] S. H. Bergens, M. E. P. Markiewicz. In *Encyclopedia of Electrochemical Power Sources*. J. Garche. Ed. Elsevier: Amsterdam, 2009 616-625.
- [16] Z. Jin, D. Nackashi, W. Lu, C. Kittrell, J. M. Tour, *Chem. Mater.*, 22, 5695 (2010).
- [17] L. Wu, L.Y. Feng, *Biosens Bioelectron.*, 34, 57 (2012).
- [18] Y. F. Xu, Z. B. Liu, X. L. Zhang, Y. Wang, J. G. Tian, Y. Huang, Y. F. Ma, X. Y. Zhang, Y. S. Chen, *Adv. Mater.*, 21, 1275 (2009).
- [19] A. Wojcik, P. V. Kamat, *ACS Nano*, 4, 6697 (2010).
- [20] N. Karousis, A. S. D. Sandanayaka, T. Hasobe, *J. Mater. Chem.*, 21, 109 (2011).
- [21] M. B. M. Krishna, N. Venkatramaiah, R. Venkatesan, D. N. Rao, *J. Mater. Chem.*, 22, 3059 (2012).
- [22] X. F. Zhang, H. J. Xu, *J. Chem. Soc., Faraday Trans.*, 89, 3347 (1993).
- [23] A. W. Snow, Phthalocyanine aggregation. In: K. M. Kadish, K. M. Smith, R. Guilard, editors. *The porphyrin handbook*. San Diego: Academic Press (2003) 129.
- [24] A. K. Geim, P. Kim, *Sci. Am.*, 4, 90 (2008).
- [25] S. K. Kim, S. Jeon, *Electrochem. Commun.*, 22, 141 (2012).
- [26] L. Q. Jiang, M. Li, L. Lin, Y. F. Li, X. Q. He, L. L. Cui, *RSC Adv.*, 4, 26653 (2014).
- [27] J. M. You, H. S. Han, H. K. Lee, S. Cho, S. Jeon, *Int. J. Hydrogen Energy*, 39, 4803 (2014).
- [28] L. L. Cui, G. J. Lv, X. Q. He, *J. Power Sources*, 282, 9 (2015).
- [29] V. Mani, R. Devasenathipathy, S. M. Chen, J. A. Gu, S. T. Huang, *Renew. Energ.*, 74, 867 (2015).
- [30] W. Lu, C. Wang, Q. Lv, X. Zhou, *J. Electroanal. Chem.*, 558 (2003).
- [31] R. S. Nicholson, I. Shain, *Anal. Chem.*, 36, 706 (1964).
- [32] A. J. Bard, L. R. Faulkner, *Electrochemical Methods-Fundamentals and Applications*, Wiley, New York, 1980 (chapters 3 and 12).
- [33] A. Fuerte, A. Cormab, M. Iglesias, E. Morales, F S'anchez, *J. Mol. Catal. A-Chem.*, 246, 109 (2006).